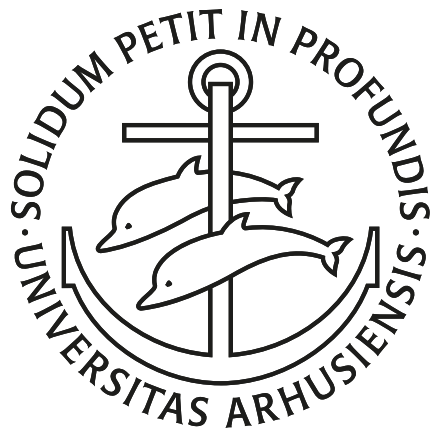

Quantum Particle in Curved Waveguides

Position-Dependent Mass Theory vs. Geometric Potential

DENMARK, JUNE 2016

BACHELOR'S THESIS
SUBMITTED BY

METTE DYBDAHL MORTENSEN
201303689
Aarhus University
Department of Physics and Astronomy



SUPERVISED BY
DMITRI FEDOROV

Abstract

This project searches to find a one-dimensional Hamiltonian to describe a single quantum particle trapped inside a curved waveguide. A simulation of the system is made in two dimensions.

Five one-dimensional Hamiltonians are built by assuming that the particle moves along a curve which can be parameterized in one dimension and introducing the position-dependent effective mass to make up for the small two-dimensional movement which must occur when the particle encounters a curve. A sixth Hamiltonian is built using a geometric potential and is tested along with the others.

It is found that for a broad waveguide the Hamiltonian with all the mass between the two differential operators might be slightly better than the others, but none of the Hamiltonians are perfect when compared to the two-dimensional simulation. For a narrow waveguide however, the results indicate that the Hamiltonian with a geometric potential describes the simulation well.

Resumé

Dette projekt forsøger at finde en endimensionel Hamiltonoperator til at beskrive en kvantepartikel fanget i en kurvet bølgeleder. En simulering af systemet opbygges i to dimensioner.

Fem endimensionelle Hamiltonoperatorer bygges ved at antage at partiklen bevæger sig langs en kurve, som kan parametriskeres i én dimension, og herefter introducere en positionsafhængig effektiv masse for at gøre op for den todimensionelle bevægelse, som må forekomme, når partiklen møder en kurve. En sjette Hamiltonoperator bygges ved brug af et geometrisk potentiiale og testes sammen med de andre.

Det viser sig, at for en bred bølgelede er Hamiltonoperatoren med alt massen placeret imellem de to differentialoperatorer måske en smule bedre end de andre, men ingen af dem er perfekte, når de sammenlignes med simuleringen. For en smal bølgelede derimod peger resultaterne på, at Hamiltonoperatoren med det geometriske potentiiale beskriver simuleringen godt.

Contents

Contents	ii
1 Introduction	1
2 The two-dimensional simulation	2
2.1 Building the simulation	2
2.2 Comparing with one dimension	5
3 The one-dimensional system	7
3.1 The position-dependent effective mass	7
3.2 The geometric potential	9
3.3 Hamiltonians	11
3.4 Building the system numerically	12
4 Results	14
4.1 The modified hyperbola f_1	14
4.2 The Gaussian f_2	16
4.3 Arctangent f_3	18
4.4 Convergence	20
5 Discussion	22
5.1 Interpretation of the results	22
5.2 Improvements and further work	22
6 Conclusion	23
Bibliography	24

Chapter 1

Introduction

It is interesting to look at the position-dependent mass as it is applicable in different fields of physics such as nuclear physics or condensed matter physics where it can be used to describe motion of holes and electrons in semiconductors of a variable chemical composition[1].

Another place where introducing a position-dependent mass might be useful is when describing motion of a single quantum particle in a curved waveguide. Quantum waveguides are important since, among other things, they can be used to describe electrons in nanowires or neutrons propagating along fibers[2]. In this project a situation with a quantum particle placed in different curved waveguides will be treated. The waveguides will be build so the motion of the particle can be described in two dimensions.

When trying to describe the same situation by using the position-dependent mass, an interesting problem of where to place the mass with respect to the Laplacian in the kinetic energy term of a Hamiltonian arises. The same problem has been treated in [3]. In this project I search to extent and improve this investigation. Firstly the two-dimensional describtion is improved by building a harmonic potential in which the perpendicular distance to the curve is used instead of the y -distance. This creates a more realistic picture of the waveguide.

In order to examine the situation further I choose to look at three waveguides built around three different curves. Another interesting thing, which I look at, is how it affects the result if the potential is sharpened and thus the waveguides become narrower.

Lastly I include a Hamiltonian with a so called geometric potential to see if this will describe the situation better than the Hamiltonians built by placing the mass differently around the differential operators.

Chapter 2

The two-dimensional simulation

I will be looking at a single quantum particle which is trapped in a waveguide and thus is constrained to move along a specific curve. A situation has been chosen where it is possible to describe the movement of this particle in two dimensions. The description will include movement along the curve as well as transverse oscillations because of a harmonic trapping potential.

As long as the particle only moves in two dimensions, it is possible for a computer to do these simulations. If the problem, however, is extended to three dimensions, it becomes increasingly difficult to solve this numerically as the matrices involved become too large for the computer to handle.

2.1 Building the simulation

When investigating this problem I have decided to look at three different curves which the waveguides will be built along. These curves are described by the following functions,

$$f_1(x) = c - \sqrt{k \cdot x^2 + 1} \quad (2.1)$$

$$f_2(x) = A + B \cdot e^{-x^2/a^2} \quad (2.2)$$

$$f_3(x) = C + \arctan(p \cdot x). \quad (2.3)$$

In f_1 the constant c determines the height of the peak of the curve and the constant k decides how sharp the curve will be. In f_2 the constant A decides an offset in the y -coordinate, the constant B determines the height of the curve's peak and a decides the sharpness of the curves. Finally in f_3 the constant C determines an offset on the y -axis and p determines the sharpness.

f_1 is a hyperbola which has been modified by shifting the coordinates and adjusting the sharpness of the peak by changing k . This function only has one curve at $x = 0$ and is therefore quite simple. Hopefully the results will be clear in this case.

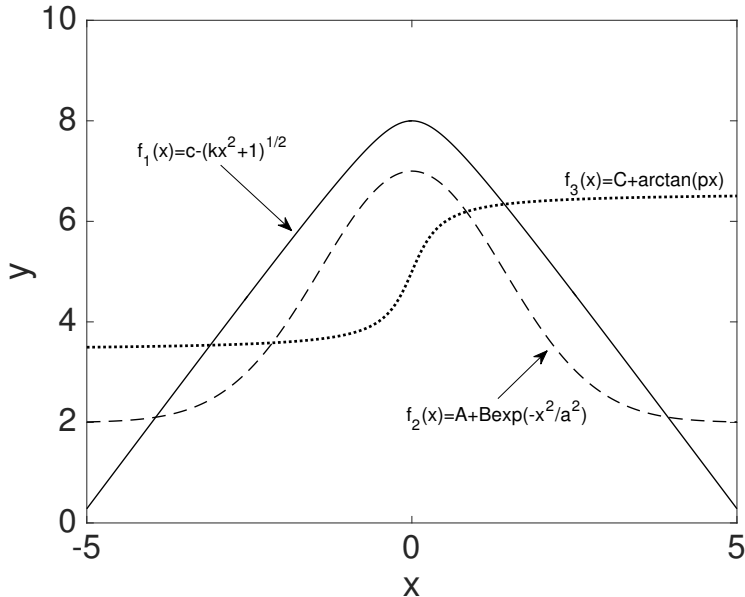


Figure 2.1: The three different curves being followed inside a quadratic box of sidelength L .

The Gaussian f_2 bends in three places which makes it a little more complex. The sharpest curve is, however, still at $x = 0$ and the results might be close to the ones for f_1 .

Lastly f_3 is the function for inverse tangent. This function has two curves. Another thing to notice is that arctangent is not symmetric with respect to the y -axis.

The particle moves inside a square box with the sidelength L which is kept the same for all three curves.

To get an idea of the difference between the three curves, they are plotted together in figure 2.1.

The time-independent Schrödinger equation in two dimensions is written as

$$\left[-\frac{\hbar^2}{2m_0} \frac{\partial^2}{\partial x^2} - \frac{\hbar^2}{2m_0} \frac{\partial^2}{\partial y^2} + V_{trap}(x, y) \right] \psi(x, y) = E\psi(x, y), \quad (2.4)$$

where V_{trap} is the trapping potential and m_0 is the mass of the particle. The 0-subscript becomes important later when the position-dependent mass is introduced. The trapping potential should be a harmonic potential of the form,

$$V_{trap} = \frac{\hbar^2}{2m_0 b^2} \frac{d^2}{b^2}, \quad (2.5)$$

where d is the perpendicular distance to the functions $f(x)$ in equations (2.1)–(2.3) and b decides the steepness of the potential. A waveguide like this is shown in figure 2.2. The waveguide in the figure follows the curve of f_1 , but the idea is the same for the two other curves.

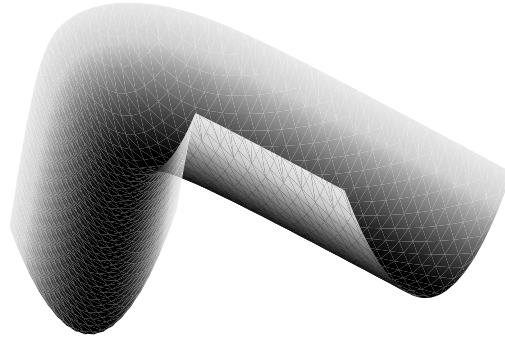


Figure 2.2: A waveguide following the function f_1 in equation (2.1) built by a harmonic potential of the form (2.5).

The simulation is done by creating a square box with sidelength L in the xy -plane and dividing each side of the box into $n - 1$ equally sized intervals. This will result in a grid with a total of $n \times n$ points.

The numerical calculations of the second derivatives in equation (2.4) are done by approximating [4]

$$\frac{\partial^2}{\partial x^2} \psi(x_i, y_j) \approx \frac{\psi(x_{i+1}, y_j) + \psi(x_{i-1}, y_j) - 2\psi(x_i, y_j)}{(\Delta x)^2}, \quad (2.6)$$

where Δx is the distance between two neighbouring points. The same approximation is made for the y -coordinates.

Since the particle should not leave the box, the wave function must be zero on the edges of the box. With this boundary condition the correlation between the rest of the point can then be described by a $(n - 2)^2 \times (n - 2)^2$ matrix M . An example of this matrix for a 5×5 grid can be seen in [3]. The equation which needs to be solved then becomes

$$M\phi = E\phi, \quad (2.7)$$

where ϕ will be a vector with $(n - 2)^2$ entries. The ϕ -vector will look like

$$\phi = \begin{bmatrix} \psi(x_2, y_2) \\ \psi(x_3, y_2) \\ \vdots \\ \psi(x_2, y_3) \\ \psi(x_3, y_3) \\ \vdots \\ \vdots \\ \psi(x_{n-1}, y_{n-1}) \end{bmatrix}, \quad (2.8)$$

where $\psi(x_i, y_j)$ is the value of the wave function in the grid-point (x_i, y_j) . The points on the grid are numbered so $i, j \in \{1, 2, \dots, n\}$.

Solving equation (2.7) is just a question of finding eigenvalues and eigenvectors of the matrix M . The eigenvectors are the different wave functions and the corresponding eigenvalues are the energies of each given state. The eigenvector with the lowest corresponding eigenvalue is of course the ground state.

After sorting the eigenvectors to match the grid and adding zeros on the edges, the wave function $\psi(x, y)$ can be plotted. These plots for the groundstate of the particle in each of the three waveguides f_1 , f_2 and f_3 can be seen in figure 2.3.

2.2 Comparing with one dimension

Later in this project these simulations in two dimensions need to be compared to different probability distributions in one dimension.

The comparison will be done in the x -coordinate as this is simplest for the given situation. It makes things quite easy because the two-dimensional simulation is in x - and y -coordinates already and all that needs to be done is integrating the probability distribution along the y -axis and making sure that the resulting probability distribution is properly normalized.

The integration is done by using the trapezoidal rule[5]. Doing the integral of the probability distribution from 0 to L on y -axis numerically will then look like

$$|\psi(x_i)|^2 = \int_0^L |\psi(x_i, y)|^2 dy \approx \frac{\Delta y}{2} \sum_{k=1}^{n-1} (|\psi(x_i, y_{k+1})|^2 + |\psi(x_i, y_k)|^2), \quad (2.9)$$

where Δy is the distance between two grid points on the y -axis. Notice that the box is quadratic and the number of intervals on each axis is the same so $\Delta y = \Delta x$.

To make sure the probability distribution is normalized correctly, $|\psi(x_i)|^2$ is divided by the integral $\int_{-L/2}^{L/2} |\psi(x)|^2 dx$, or numerically,

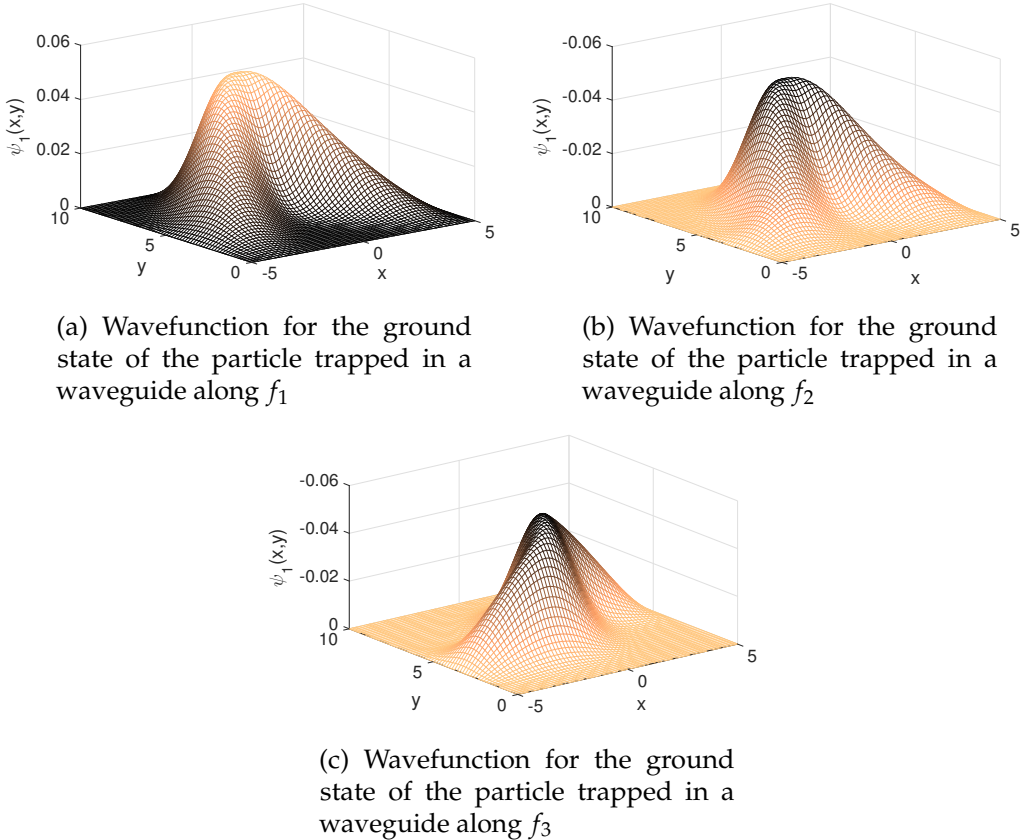


Figure 2.3: The wave function of the ground state for the three different curves. The sign of the wave function is not important as only the probability distribution will be used in the later comparison.

$$|\psi(x_i)|^2 = \frac{|\psi(x_i)|^2}{\frac{\Delta x}{2} \sum_{k=1}^{n-1} (|\psi(x_{k+1})|^2 + |\psi(x_k)|^2)}. \quad (2.10)$$

In the end we will have a nicely normalized probability distribution $|\psi(x)|^2$ in x -coordinates ready for the later comparison.

Chapter 3

The one-dimensional system

I will now try to describe the same problem in one dimension. The motivation for doing this is that if the same system can be described in one dimension, problems like this become much easier for a computer to solve. It is unfortunately not clear exactly how the problem should be translated into one dimension.

When building the one-dimensional systems it is assumed that the particle only moves along the curve and does not make transverse oscillations. That is, the movement can be described in one dimension rather than two. This assumption will be alright if the particle is sufficiently cooled. Even so when the particle encounters a curve in the waveguide it must go up the sides of the potential a little. To make up for this kind of two-dimensional movement one can try introducing a position-dependent mass.

When doing the simulation the curve being followed should be parameterized in one dimension. One way of doing this is by parameterizing by arc length with the parameter s . For the curves in equation (2.1)-(2.3) this is however not the simplest way as $s(x)$ is found by solving an integral which can not be solved analytically for any of the three curves. Therefore I have chosen to just use the parameter x directly. This choice also makes it simpler to do the later comparison.

3.1 The position-dependent effective mass

One theory on how to describe the situation in one dimension is the so called position-dependent mass theory.

When using this method one starts out by looking at the kinetic energy for two-dimensional motion. By translating this so only one parameter x appears, we will get an expression from which it is natural to define a position-dependent effective mass.

Classical kinetic energy is given by

$$\begin{aligned} T &= \frac{1}{2}m_0(\dot{x}^2 + \dot{y}^2) \\ &= \frac{1}{2}m_0 \left[1 + \left(\frac{dy}{dx} \right)^2 \right] \dot{x}^2. \end{aligned} \quad (3.1)$$

Here $y = f(x)$ are the functions in equation (2.1)–(2.3) and the dots mark the derivatives with respect to time as usual.

This helps define an effective mass which now becomes dependent on the position x . Expressed in x -coordinates this is

$$m(x) = m_0 \cdot \left(1 + (f'(x))^2 \right), \quad (3.2)$$

where $f'(x)$ is the derivative of the curve with respect to x and m_0 is the actual mass of the particle which was also used in the two-dimensional simulation.

Because this effective mass depends on the position x , it raises the question of how to quantize the problem. The issue is that it is not obvious where to place the mass with respect to the Laplace operator in the Hamiltonian. Writing down a general form of the Hamiltonian and not yet deciding on where to place the mass will give us [1]

$$H = -\frac{\hbar^2}{4} \cdot \left(\frac{1}{m^\alpha} \frac{\partial}{\partial x} \frac{1}{m^\beta} \frac{\partial}{\partial x} \frac{1}{m^\gamma} + \frac{1}{m^\gamma} \frac{\partial}{\partial x} \frac{1}{m^\beta} \frac{\partial}{\partial x} \frac{1}{m^\alpha} \right), \quad (3.3)$$

where $m = m(x)$ and we of course must have $\alpha + \beta + \gamma = 1$ to get all of the units right. Building the Hamiltonian in this way ensures that it becomes Hermitian even if we choose $\alpha \neq \gamma$.

The evaluation of the operators in equation (3.3) proceeds as follows where defining $m = m(x)$ and $\psi = \psi(x)$ makes the notation slightly shorter,

$$\begin{aligned} \frac{\partial}{\partial x} \frac{1}{m^\gamma} \psi &= -\gamma \frac{m'}{m^{\gamma+1}} \psi + \frac{1}{m^\gamma} \frac{\partial \psi}{\partial x} & (3.4) \\ \frac{1}{m^\alpha} \frac{\partial}{\partial x} \frac{1}{m^\beta} \frac{\partial}{\partial x} \frac{1}{m^\gamma} &= -\gamma \frac{m''}{m^2} \psi + \gamma(\gamma + \beta + 1) \frac{m'^2}{m^3} \psi \\ &\quad - \gamma \frac{m'}{m^2} \frac{\partial \psi}{\partial x} - (\gamma + \beta) \frac{m'}{m^2} \frac{\partial \psi}{\partial x} + \frac{1}{m} \frac{\partial^2 \psi}{\partial x^2} \\ &= -\gamma \frac{m''}{m^2} \psi - (\alpha\gamma - 2\gamma) \frac{m'^2}{m^3} \psi \\ &\quad + (\alpha - \gamma - 1) \frac{m'}{m^2} \frac{\partial \psi}{\partial x} + \frac{1}{m} \frac{\partial^2 \psi}{\partial x^2}. & (3.5) \end{aligned}$$

Here $\alpha + \beta + \gamma = 1$ has been used repeatedly. This was for the first term in equation (3.3). The second term will be similar with γ 's replaced by α 's.

When collecting all the terms the following Hamiltonian will be obtained,

$$H = -\frac{\hbar^2}{2} \left(\frac{1}{m(x)} \frac{\partial^2}{\partial x^2} - \frac{m'(x)}{(m(x))^2} \frac{\partial}{\partial x} \right) + V_{eff}, \quad (3.6)$$

where V_{eff} is an effective potential given by

$$V_{eff} = -\frac{\hbar^2}{4} \left((2\alpha + 2\gamma - 2\alpha\gamma) \frac{(m'(x))^2}{(m(x))^3} - (\alpha + \gamma) \frac{m''(x)}{(m(x))^2} \right), \quad (3.7)$$

and $m'(x)$ and $m''(x)$ are the first and second derivative of the mass with respect to the position x . It is worth noticing that only the effective potential depends on the choice of α , β and γ while the first part of the (3.6) will be the same for the different Hamiltonians.

Now the challenge is choosing α, β and γ so that the model will be most succesfull when it comes to describing the two-dimensional simulation.

In this project I have chosen to look at the following five cases,

Case 1: $\alpha = \gamma = \frac{1}{2}, \beta = 0$

Case 2: $\alpha = \gamma = \frac{1}{4}, \beta = \frac{1}{2}$

Case 3: $\alpha = \gamma = \frac{1}{6}, \beta = \frac{2}{3}$

Case 4: $\alpha = \gamma = 0, \beta = 1$

Case 5: $\alpha = 1, \beta = \gamma = 0$

This results in five different Hamiltonians which will be summarized later in section 3.3.

3.2 The geometric potential

Varying the values of α , β and γ in equation (3.3) is one way of dealing with the problem. Another approach is including a so called geometric potential. This will give another Hamiltonian which can not be acchieved by choosing a special combination of α , β and γ .

The geometric potential is attractive and proportional to the curvature κ squared. An analog can be drawn from the approximations made for the geometric potential to the ones from the Born-Oppenheimer approximation in molecular physics [2].

If the curve being followed is parameterized by arc length s , the Hamiltonian simply becomes [6]

$$H = -\frac{\hbar^2}{2m_0} \frac{\partial^2}{\partial s^2} + V_{geo}, \quad (3.8)$$

where the geometric potential V_{geo} is defined as

$$V_{geo} = -\frac{\hbar^2 \kappa^2}{8m_0}, \quad (3.9)$$

and the curvature κ of a curve $y = f(x)$ can be found with the formula [7],

$$\kappa = \frac{y''}{(1+y'^2)^{3/2}}. \quad (3.10)$$

Since so far I have been working with x -coordinates, a change from s - to x -coordinates must be made before this Hamiltonian can be used in comparison with the others.

When letting $u(s)$ be the wave function in s -coordinates, translating to x -coordinates, and using the product rule, the second derivative in (3.8) becomes

$$\begin{aligned} \frac{\partial^2 u(s)}{\partial s^2} &= \frac{\partial}{\partial s} \left(\frac{\partial u(s(x))}{\partial x} \frac{\partial x}{\partial s} \right) \\ &= \frac{\partial}{\partial x} \left(\frac{\partial u(s(x))}{\partial x} \frac{\partial x}{\partial s} \right) \frac{\partial x}{\partial s}. \end{aligned} \quad (3.11)$$

Now since $ds^2 = dx^2 + dy^2$, we have $ds = \sqrt{1 + \left(\frac{dy}{dx}\right)^2} dx = \sqrt{\frac{m(x)}{m_0}} dx$, where $m(x)$ is taken from equation (3.2). This results in

$$\frac{\partial^2 u(s)}{\partial s^2} = \sqrt{\frac{m_0}{m(x)}} \frac{\partial}{\partial x} \left(\sqrt{\frac{m_0}{m(x)}} \frac{\partial}{\partial x} \right) u(s(x)). \quad (3.12)$$

Substituting this into the Schrödinger equation $Hu = Eu$, where H is the Hamiltonian from equation (3.8), we get

$$\left(-\frac{\hbar^2}{2} \frac{1}{\sqrt{m(x)}} \frac{\partial}{\partial x} \frac{1}{\sqrt{m(x)}} \frac{\partial}{\partial x} + V_{geo} \right) u(s(x)) = Eu(s(x)). \quad (3.13)$$

It is important to remember that the wave function should be normalized correctly. That is

$$\begin{aligned} 1 &= \int |u(s)|^2 ds = \int |u(s(x))|^2 \sqrt{m(x)/m_0} dx \\ &= \int |(m(x)/m_0)^{1/4} u(s(x))|^2 dx. \end{aligned} \quad (3.14)$$

When taking this into account the wave function must be defined as $\psi(x) = (m(x)/m_0)^{1/4} u(s(x))$. Introducing this in the Schrödinger equation leads to

$$\begin{aligned} \left(-\frac{\hbar^2}{2} \frac{1}{\sqrt{m(x)}} \frac{\partial}{\partial x} \frac{1}{\sqrt{m(x)}} \frac{\partial}{\partial x} \left(\frac{m_0}{m(x)} \right)^{1/4} + \frac{V_{geo}}{(m(x)/m_0)^{1/4}} \right) \psi(x) \\ = E \frac{\psi(x)}{(m(x)/m_0)^{1/4}}, \end{aligned} \quad (3.15)$$

and by multiplying both sides with $(m(x)/m_0)^{1/4}$, the resulting Hamiltonian becomes

$$H_{geo} = -\frac{\hbar^2}{2} \frac{1}{m(x)^{1/4}} \frac{\partial}{\partial x} \frac{1}{\sqrt{m(x)}} \frac{\partial}{\partial x} \frac{1}{m(x)^{1/4}} + V_{geo}. \quad (3.16)$$

Notice that this corresponds to Case 2 where $\alpha = \gamma = \frac{1}{4}$ and $\beta = \frac{1}{2}$ with an addition to the effective potential in the form of the geometric potential V_{geo} .

The Hamiltonian is still one dimensional and now also in the x -coordinate, thus the same approach as for the other one-dimensional Hamiltonians can be used when finding the wave function.

3.3 Hamiltonians

All in all the different one-dimensional Hamiltonians that will be tested in this project are the following,

$$H_1 = -\frac{\hbar^2}{2} \frac{1}{\sqrt{m(x)}} \frac{\partial^2}{\partial x^2} \frac{1}{\sqrt{m(x)}} \quad (3.17)$$

$$H_2 = -\frac{\hbar^2}{2} \frac{1}{(m(x))^{\frac{1}{4}}} \frac{\partial}{\partial x} \frac{1}{\sqrt{m(x)}} \frac{\partial}{\partial x} \frac{1}{(m(x))^{\frac{1}{4}}} \quad (3.18)$$

$$H_3 = -\frac{\hbar^2}{2} \frac{1}{(m(x))^{\frac{1}{6}}} \frac{\partial}{\partial x} \frac{1}{(m(x))^{\frac{2}{3}}} \frac{\partial}{\partial x} \frac{1}{(m(x))^{\frac{1}{6}}} \quad (3.19)$$

$$H_4 = -\frac{\hbar^2}{2} \frac{\partial}{\partial x} \frac{1}{m(x)} \frac{\partial}{\partial x} \quad (3.20)$$

The idea with these four Hamiltonians is that all of the mass starts on either side of the differential operators in H_1 and moves towards the middle, so that in H_4 all the mass is placed between the two operators.

Furthermore I have chosen to also use one Hamiltonian where the mass is not placed symmetrically around the operators. This one is

$$H_5 = -\frac{\hbar^2}{4} \left(\frac{1}{m(x)} \frac{\partial^2}{\partial x^2} + \frac{\partial^2}{\partial x^2} \frac{1}{m(x)} \right) \quad (3.21)$$

Lastly I have looked at a Hamiltonian where a geometric potential has been included. As shown above, this corresponds to H_2 with an additional part to the potential in form of V_{geo} .

$$H_{geo} = -\frac{\hbar^2}{2} \frac{1}{(m(x))^{\frac{1}{4}}} \frac{\partial}{\partial x} \frac{1}{\sqrt{m(x)}} \frac{\partial}{\partial x} \frac{1}{(m(x))^{\frac{1}{4}}} + V_{geo} \quad (3.22)$$

When doing the calculations all of the Hamiltonians should be written out by using the expression from equation (3.6).

3.4 Building the system numerically

When building the one-dimensional systems the same kind of approach as for the two-dimensional system is used.

Now only working with the x -axis, the same trick of dividing the axis into $n - 1$ equally sized intervals is performed. This will result in n equally spaced points x_1, x_2, \dots, x_n at which the wave function should be determined.

Numerically the first and second derivatives of the wave function are approximated by [4]

$$\frac{\partial}{\partial x} \psi(x_i) \approx \frac{\psi(x_{i+1}) - \psi(x_{i-1})}{2 \cdot \Delta x} \quad (3.23)$$

$$\frac{\partial^2}{\partial x^2} \psi(x_i) \approx \frac{\psi(x_{i+1}) + \psi(x_{i-1}) - 2\psi(x_i)}{(\Delta x)^2}, \quad (3.24)$$

where Δx is the length of each of the $n - 1$ intervals. As with the two dimensional approach, this results in a matrix problem which should be solved by finding eigenvalues and eigenvectors.

The eigenvector with the lowest corresponding eigenvalue will be the wave function of the ground state. The eigenvector with the second lowest eigenvalue will be the wave function of the first excited state and so forth.

When the wave functions have been found, they need to be normalized so the comparison between the probability distributions can be done accordingly.

The normalization is done by dividing the probability distribution by the integral of the probability distribution. The integral is done numerically by using the trapezoidal rule in the same way as in equation (2.10).

Chapter 4

Results

During the investigation the following values of the different constants have been used: $\hbar = 1$ in units of energy times time, $m_0 = 1$ in units of mass, $L = 10$ in units of length, and $n = 65$. The value of b in the potential (2.5) has been varied to see how the results differ if the potential becomes steeper.

For each of the three different waveguides the first three states have been considered. For each of these three states two values of b have been used. These values are $b = 1$ and $b = \frac{1}{3}$

4.1 The modified hyperbola f_1

The results for the ground state of the particle in the f_1 -waveguide can be seen in figure 4.1.

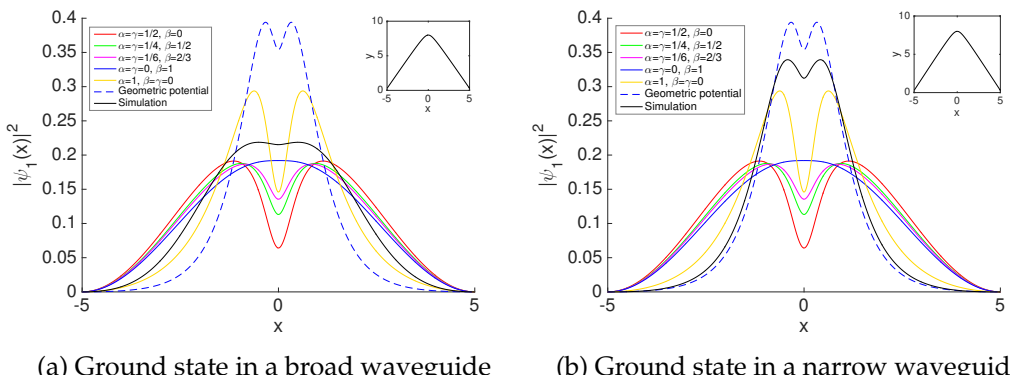


Figure 4.1: Probability distributions of the ground state for a particle in respectively a broad and a narrow waveguide shaped along f_1

Looking at the probability distributions of the ground state in figure 4.1a where $b = 1$ makes the trapping potential broad, it is clear that none of the one-dimensional descriptions fit the simulation perfectly. It is a little hard to see if one of them is better

than the others. The probability distributions corresponding to the Hamiltonian with the geometric potential H_{geo} (blue dashed) and the Hamiltonian H_5 with $\alpha = 1$, $\beta = \gamma = 0$ (yellow) seem to have a little too tall peaks compared to the one for the simulation.

The Hamiltonian with all the mass between the operators, $\alpha = \gamma = 0$, $\beta = 1$ (blue), might be somewhat better at around $x = 0$ because the other probability distributions have too deep a local minimum.

In figure 4.1b the potential has been made narrower by setting $b = \frac{1}{3}$. This change in the potential seems to make the probability distribution of the simulation more concentrated around $x = 0$. For this more narrow waveguide it looks like the Hamiltonian with the geometric potential H_{geo} (blue dashed) is not very far off and actually provides the best description.

In figure 4.2 the results for the first excited state with the two choices of b are shown.

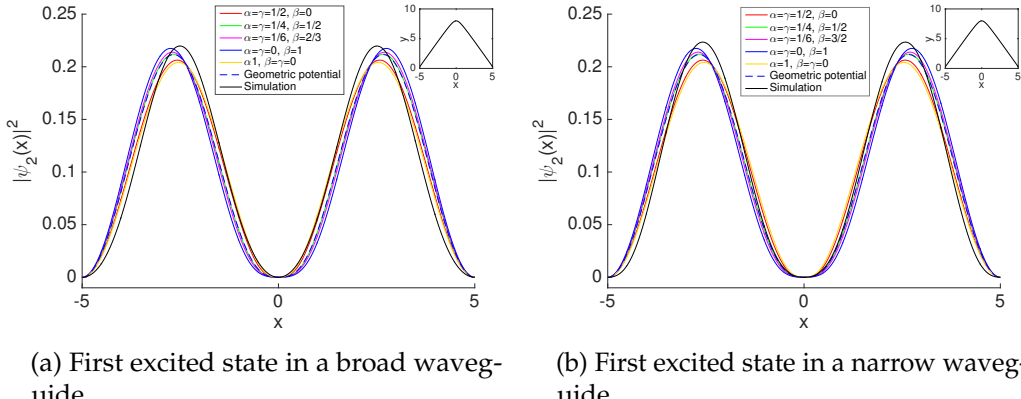


Figure 4.2: Probability distributions of the first excited state for a particle in respectively a broad and a narrow waveguide shaped along f_1

For the first excited state with the broad potential in figure 4.2a it is even harder to pick one Hamiltonian which gives a better probability distribution. Since all the probability distributions including the one for the simulation are zero at $x = 0$, which is where the peak of the curve is, it becomes difficult tell them apart. All of them generally seem to follow the shape of the probability distribution of the simulation nicely.

As seen in figure 4.2b sharpening the potential here has very little effect and the situation is the same with the probability distributions all being zero at $x = 0$.

Finally the results of the second excited state are shown in figure 4.3.

The probability distributions of the second excited state for $b = 1$ in figure 4.3a all seem off compared to the simulation. The probability distributions for the one dimensional Hamiltonians all have two zeros more than the one for the simulation.

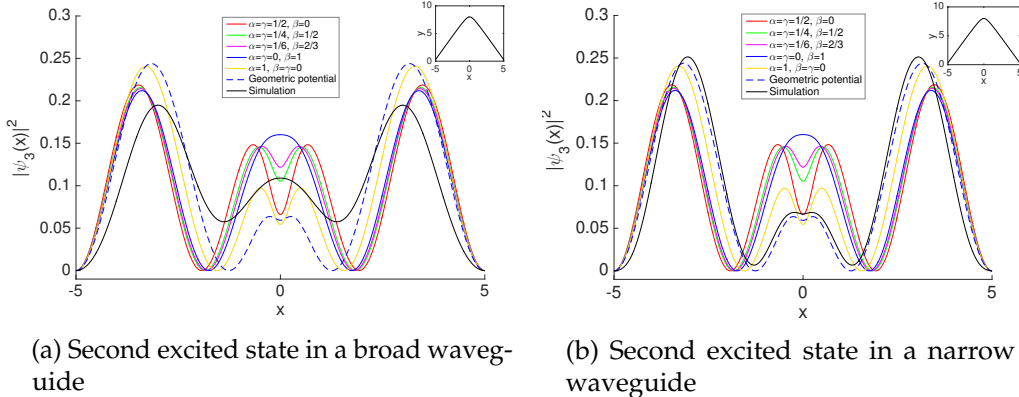


Figure 4.3: Probability distributions of the second excited state for a particle in respectively a broad and a narrow waveguide shaped along f_1

The probability distribution for the simulation has two local minima around the zeros of the probability distributions of H_5 with $\alpha = 1, \beta = \gamma = 0$ (yellow) and H_{geo} with the geometric potential (blue dashed). However, these two Hamiltonians still describe the simulation poorly.

For the narrower waveguide (figure 4.3b) the same tendency as for the ground state is apparent as the probability distribution of the simulation seems to move closer to the one associated with the Hamiltonian with geometric potential H_{geo} (blue dashed). It seems as if H_{geo} also describes the second excited state well for narrow waveguides .

4.2 The Gaussian f_2

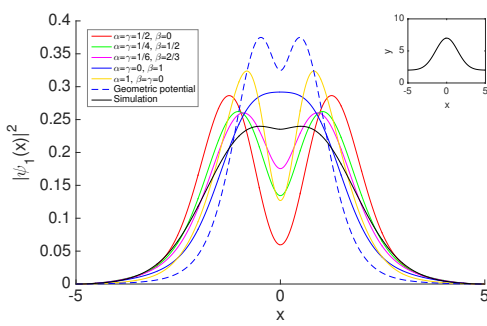
The results for the ground state of a particle trapped in a waveguide in the shape of f_2 can be seen in figure 4.4.

The results for the Gaussian curve look somewhat similar to the ones for the modified hyperbola. This is not so surprising since the shape of the curves does not differ significantly.

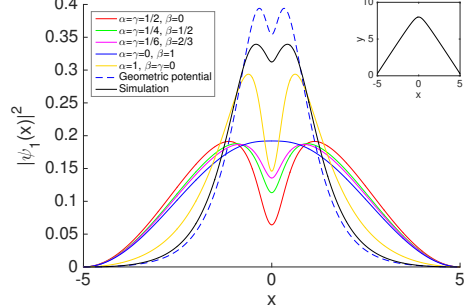
The ground state with $b = 1$ is shown in figure 4.4a. Here the peaks of all the probability distributions corresponding to the one-dimensional Hamiltonians are too tall when compared to the probability distribution of the simulation. At the same time most of the local minima at $x = 0$ are too low.

It is difficult to say if one Hamiltonian is better than the others. However H_1 with $\alpha = \gamma = \frac{1}{2}, \beta = 0$ (red), H_5 with $\alpha = 1, \beta = \gamma = 0$ (yellow) and H_{geo} (blue dashed) seem to be a little more off than the rest.

Like for the curve of f_1 , the narrower potential (seen in figure 4.4b) causes the probability distribution of the simulation to become more concentrated around



(a) Ground state in a broad waveguide

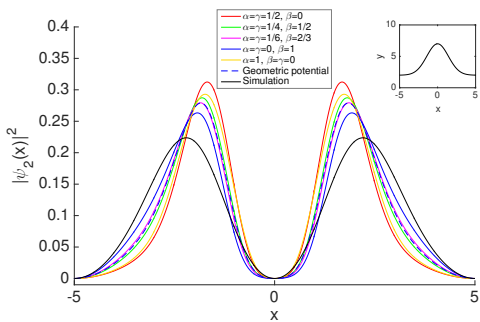


(b) Ground state in a narrow waveguide

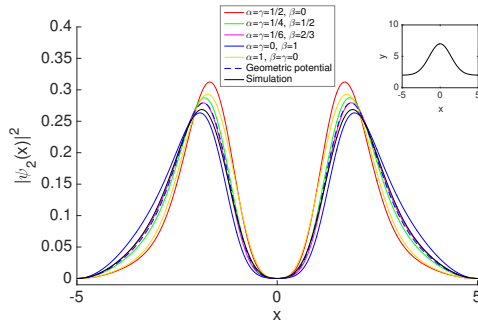
Figure 4.4: Probability distributions of ground state for a particle in respectively a broad and a narrow waveguide shaped along f_2

$x = 0$. And once again H_{geo} (blue dashed) seems to give an alright description.

The results for the first excited state can be seen in figure 4.5.



(a) First excited state in a broad waveguide



(b) First excited state in a narrow waveguide

Figure 4.5: Probability distributions of the first excited state for a particle in respectively a broad and a narrow waveguide shaped along f_2

For the first excited state with the broad potential in figure 4.5a the probability distributions all agree on being zero in $x = 0$. It is a little easier to tell them apart than for f_1 . This is probably due to the Gaussian bending in three places.

This time it is easy to see that the probability distribution related to H_4 with $\alpha = \gamma = 0, \beta = 1$ (blue) lies closest to the one for the simulation most of the time. The consistency between them is still not very good though.

For the narrower waveguide the probability distributions of the second excited state can be seen in figure 4.5b. The shape of the probability distribution of the simulation now looks more similar to the others. It now lies even closer to H_4 (blue),

but like for the ground state it has also moved closer to H_{geo} (blue dashed).

In figure 4.6 the results for the second excited state are shown.

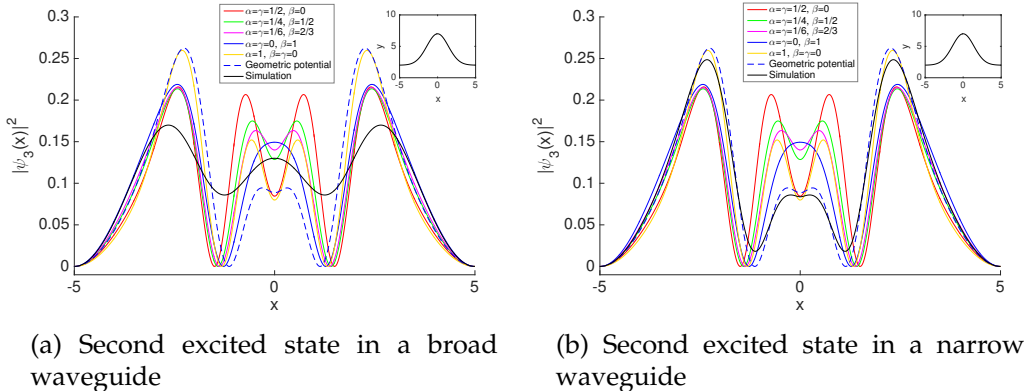


Figure 4.6: Probability distributions of the second excited state for a particle in respectively a broad and a narrow waveguide shaped along f_2

Like for the curve f_1 the probability distributions of second excited state for a broad waveguide in figure 4.6a are all off in comparison to the probability distribution of the simulation. The probability distribution of the simulation has local minima at around the points where the other probability distributions are zero.

The probability distributions of the second excited state for a narrower waveguide are shown in figure 4.6b. As seen for most of the results so far, also here the tendency is that the probability distribution of the simulation moves closer to the one of H_{geo} (blue dashed) when the potential is made steeper.

4.3 Arctangent f_3

The results for the ground state of a particle trapped in a waveguide shaped after f_3 can be seen in figure 4.7.

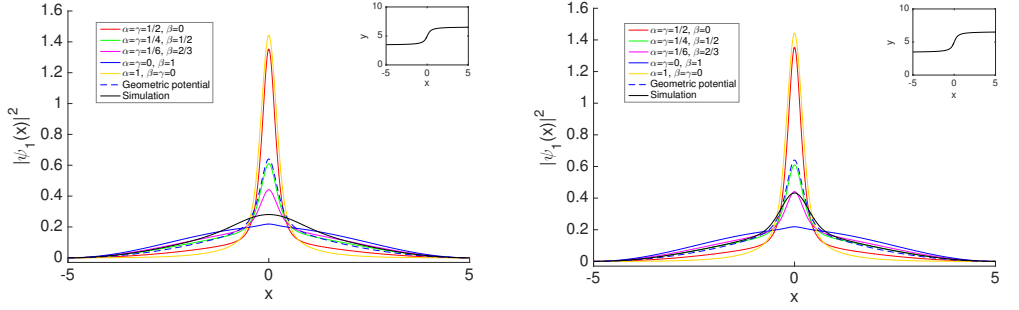


Figure 4.7: Probability distributions of the ground state for a particle in respectively a broad and a narrow waveguide shaped along f_3

The results for the arctangent curve look considerably different than for the two other curves. But the curve itself also differs a lot from the others, so it is not too surprising. The two curves of the arctangent waveguide are also not as sharp as the curves at $x = 0$ for the other two functions.

For the ground state with the broad potential in figure 4.7a the probability distribution related to H_4 with $\alpha = \gamma = 0, \beta = 1$ (blue) seems to fit the probability distribution of the simulation a bit better than the others. Most of the probability distribution are too concentrated at around $x = 0$.

When the potential is sharpened in figure 4.7b the probability distribution of the simulation becomes more concentrated around $x = 0$. It now lies close to the probability distribution related to the Hamiltonian H_3 with $\alpha = \gamma = \frac{1}{6}, \beta = \frac{2}{3}$ (magenta), but has meanwhile also moved a little closer to the other probability distributions with a high peak at $x = 0$.

The results for the first excited state are shown in figure 4.8.

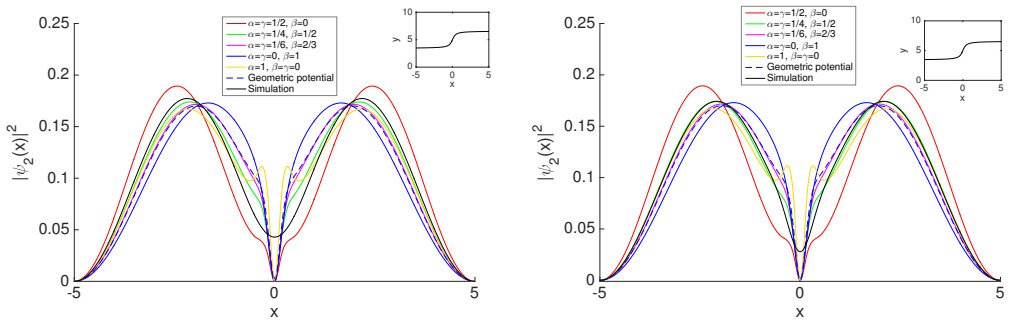


Figure 4.8: Probability distributions of the first excited state for a particle in respectively a broad and a narrow waveguide shaped along f_3

For the first excited state with a broad potential in figure 4.8a the probability distributions related to the one-dimensional Hamiltonians are all zero at $x = 0$. The one for the simulation, on the other hand, is not zero. This is due to the function f_3 not being symmetric about the y -axis. When looking past this H_2 with $\alpha = \gamma = \frac{1}{4}$, $\beta = \frac{1}{2}$ (green) might be a slightly better choice as this probability distribution mostly lies close to the one for the simulation.

When the potential becomes steeper (figure 4.8b), the probability distribution of the simulation moves slightly closer to H_2 (green), but the change is not very noticeable.

In figure 4.9 the results for the second excited state are shown.

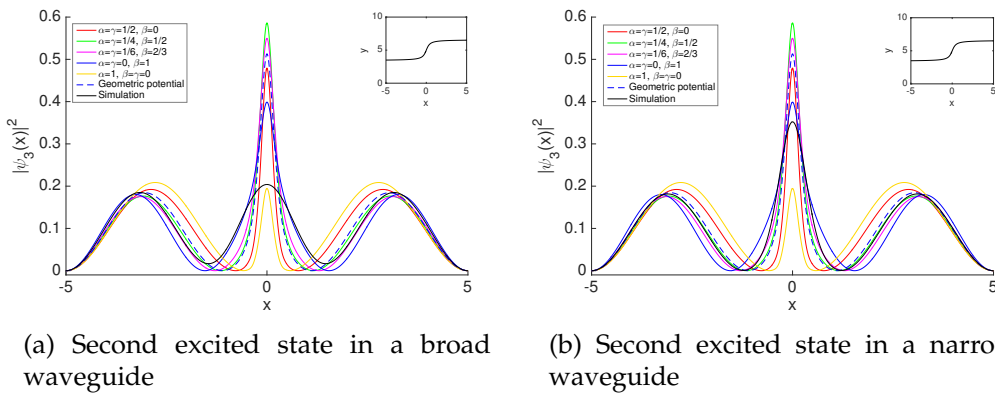


Figure 4.9: Probability distributions of the second excited state for a particle in respectively a broad and a narrow waveguide shaped along f_3

The probability distributions for the second excited state in a broad waveguide are shown in figure 4.9a. As for the ground state most of the probability distributions for the one dimensional Hamiltonians have a too tall peak at $x = 0$ when compared to the simulation. At other points however H_5 with $\alpha = \gamma = 0$, $\beta = 1$ (blue) follows the simulation pretty closely. But it is still not perfect and it might not be better than the others as it is a little hard to tell by looking at the results qualitatively.

The results for a narrower waveguide are shown in figure 4.9b. The peak of the probability distribution for the simulation at $x = 0$ has now moved closer to the one for the Hamiltonian H_5 (blue).

4.4 Convergence

It might be relevant to look at how the probability distributions converge. Working with too few points will not reproduce the right results as the numerical approximations in equations (2.6), (3.23) and (3.24) all has an error which is of the order $(\Delta x)^2$ [4]. The trapezoidal rule which is used for the numerical integration also

gives an error. Locally this error of the order of $(\Delta x)^3$ [5]. Clearly these errors will all decrease as the number of points n increase and should show a nice convergence.

I have checked the convergence for the probability distribution of the ground state of the simulation. The result of this can be seen in figure 4.10. Notice that cubic spline interpolation has been used when plotting the probability distributions which is the reason that for $n = 9$ the graph seems to go a little below 0 at the points near the edge of the box. This is of course not very nice for a probability distribution and when using cubic spline, n should be chosen high enough so that this effect will not occur.

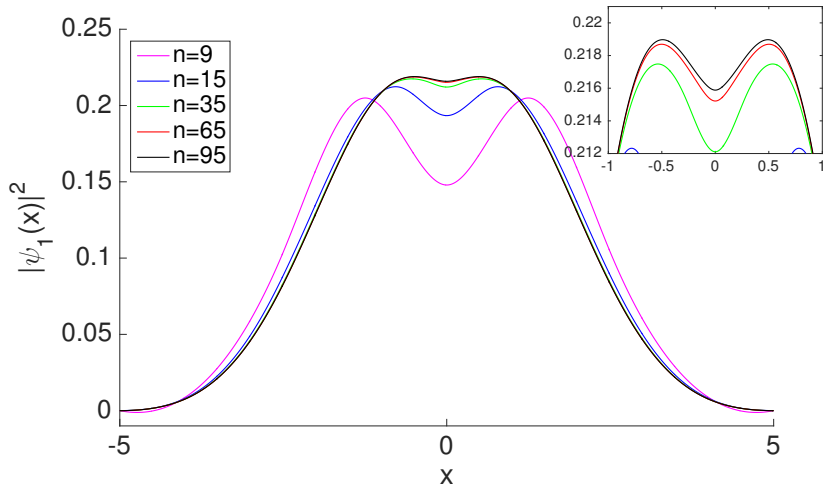


Figure 4.10: The probability distribution of the ground state of the simulation using different numbers of grid-points. In the upper right corner is a zoom of the results for $n = 35$, $n = 65$ and $n = 95$

In my investigation I have chosen to use $n = 65$ which seems reasonable when looking at figure 4.10.

Chapter 5

Discussion

5.1 Interpretation of the results

For the broad potentials it is difficult to choose a one-dimensional Hamiltonian which describes the situation better than the others. The Hamiltonian with all the mass in between the differential operators (blue in the figures) might overall be a better choice for a broad waveguide as it does not lie too far off for most of the cases. It is still far from perfect however.

For narrow waveguide it seems as if the Hamiltonian with the geometric potential (blue dashed in the figures) is generally not a bad choice. For the modified hyperbola and the Gaussian it seems to describe the situation best while there might also be other candidates for the inverse tangent curve.

5.2 Improvements and further work

From what my results show, it might be interesting to do further investigation on the Hamiltonian with the geometric potential as this has proven quite successful for narrow waveguides – at least for the two curves f_1 and f_2 .

It might also be relevant to look at the energy of the simulation compared to the energies of the situations described by the different one-dimensional Hamiltonians to see if this brings forth some additional information.

It is possible to get a better convergence with the same number of points n if the box is made smaller. When making the box smaller, however, one needs to keep in mind that the potential also needs to be made steeper in order to still have the particle following the curve.

Chapter 6

Conclusion

In this report I have done a further investigation on some problems similar to the ones in [3].

A system has been build numerically in two dimensions in which a particle moves in a quantum waveguide. Three differently curved waveguides have been used. Further more the harmonic trapping potential has been varied to see if the wavefunction of the particle changes when it moves in a narrower waveguide.

The hope was to find a nice one-dimensional describtion of the two-dimensional system. In the search for this kind of describtion the approximation has been made that the particle only moves along the curve, that is in the very bottom of the waveguide, and does not make transverse oscillations.

These assumptions have resulted in an expression for a position-dependent mass. Five different Hamiltonians, in which this mass is placed differently with respect to the differential operators, have been tested. The results have been compared to the ones for the two-dimensional simulation.

Also a sixth one-dimensional Hamiltonian has been included in the comparison. This Hamiltonian has been built using a geometric potential which depends on the curvature of the waveguides and therefore can not be obtained by simply placing the mass differently in one of the previous Hamiltonians.

The results have shown that for a broad waveguide none of the Hamiltonians give a correct describtion of the two-dimensional system. The Hamiltonian with all the mass in between the differential operators might be a slightly better choice though.

For a narrower waveguide it seemed that the Hamiltonian with a geometric potential gave an alright describtion. It would be interesting to investigate this further to see if this is true for other curves as well. For the arctangent it might already fail a little.

Bibliography

- [1] Oldwig von Roos. "Position-dependent effective masses in semiconductor theory". In: *Phys. Rev. B* 27 (12 1983), pp. 7547–7552. DOI: [10.1103/PhysRevB.27.7547](https://doi.org/10.1103/PhysRevB.27.7547). URL: <http://link.aps.org/doi/10.1103/PhysRevB.27.7547>.
- [2] J. Stockhofe and P. Schmelcher. "Nonadiabatic couplings and gauge-theoretical structure of curved quantum waveguides". In: *Phys. Rev. A* 89 (3 2014), p. 033630. DOI: [10.1103/PhysRevA.89.033630](https://doi.org/10.1103/PhysRevA.89.033630). URL: <http://link.aps.org/doi/10.1103/PhysRevA.89.033630>.
- [3] K.K Rønnow. "Numerical analysis of position-dependent effective mass Schrödinger equation". Bachelor's thesis. Aarhus University, Department of Physics and Astronomy, 2015.
- [4] *Wikibook on Numerical Methods/Numerical Differentiation*. 2015. URL: https://en.wikibooks.org/wiki/Numerical_Methods/Numerical_Differentiation.
- [5] *Wikipedia entry on the Trapezoidal Rule*. 2016. URL: https://en.wikipedia.org/wiki/Trapezoidal_rule.
- [6] J.K. Pedersen. "Classical and Quantum Behavior of Dipoles on a Helix". PhD thesis. Aarhus University, Department of Physics and Astronomy, 2015.
- [7] *Wikipedia entry on Curvature*. 2016. URL: <https://en.wikipedia.org/wiki/Curvature>.